

Reinforcement Learning for Enhancing Sensing Estimation in Bistatic ISAC Systems with UAV Swarms

Obed Morrison Atsu, Salmame Naoumi, Roberto Bomfin, Marwa Chafii

Abstract—This paper introduces a novel Multi-Agent Reinforcement Learning (MARL) framework to enhance integrated sensing and communication (ISAC) networks using unmanned aerial vehicle (UAV) swarms as sensing radars. By framing the positioning and trajectory optimization of UAVs as a Partially Observable Markov Decision Process, we develop a MARL approach that leverages centralized training with decentralized execution to maximize the overall sensing performance. Specifically, we implement a decentralized cooperative MARL strategy to enable UAVs to develop effective communication protocols, therefore enhancing their environmental awareness and operational efficiency. Additionally, we augment the MARL solution with a transmission power adaptation technique to mitigate interference between the communicating drones and optimize the communication protocol efficiency. Moreover, a transmission power adaptation technique is incorporated to mitigate interference and optimize the learned communication protocol efficiency. Despite the increased complexity, our solution demonstrates robust performance and adaptability across various scenarios, providing a scalable and cost-effective enhancement for future ISAC networks.

Index Terms—Multi-agent reinforcement learning (MARL), Integrated sensing and communication (ISAC), Unmanned aerial vehicle (UAV).

I. INTRODUCTION

Within the emerging landscape of 6G systems, integrated sensing and communication (ISAC) has been identified as a key technology shaping the future of wireless systems. ISAC represents an innovative framework that enables the development of spectrally coexistent communication and sensing functionalities, thereby enhancing spectrum efficiency and reducing hardware and computational resource costs [1]. Communication-centric ISAC is a major area of research, aiming to add opportunistic sensing capabilities to existing communication infrastructures. This approach focuses on meeting communication application requirements while estimating sensing parameters from communication waveforms reflected off objects in the environment, effectively repurposing the channel estimation process [2]. Pertinent to communication-centric ISAC networks

is the use of sensing receivers in two primary configurations, either monostatic or decentralized. Decentralized configurations, such as bistatic or multi-static setups, involve passive radars that are separately placed with the aim of localizing and tracking targets in the environment without disrupting the existing communication infrastructure. These configurations have shown significant promise in practical settings compared to monostatic systems, which often experience high self-interference leakage [3]. However, several challenges, such as asynchrony, limited visibility, high double path loss, and blind spots, hinder the practical application of ISAC in decentralized settings. Therefore, integrating non-terrestrial components, such as unmanned aerial vehicles (UAVs), into terrestrial ISAC networks is a promising approach to overcome these issues.

Recently, there has been growing interest from both industry and academia in integrating UAVs into future mobile infrastructure due to their potential to revolutionize networks and enhance a wide range of applications, from emerging 6G use cases to critical military and public safety operations [4]. Moreover, UAVs offer dynamic reconfigurability, adaptability, cost-effectiveness, and rapid deployment, making them ideal for communication-centric ISAC applications, including real-time monitoring and public safety operations such as search-and-rescue missions [5]. Several studies have explored the use of UAVs to enhance wireless networks. For example, [6] proposed deploying a UAV to provide wireless coverage for indoor users in high-rise buildings during disaster situations. [7] investigated trajectory planning for rescue relief tasks and introduced a deep reinforcement learning algorithm based on intrinsic rewards to maximize communication coverage for mobile users. In the specific context of ISAC, [8] proposed an extended Kalman filtering-based tracking scheme for a UAV-enabled ISAC system, where a UAV tracks a moving object while also communicating with a device attached to it. The work in [9] introduced a multi-agent reinforcement learning (MARL) framework that leverages emergent communication strategies for the effective deployment of UAVs in ISAC settings. Additionally, [10] proposed a framework for UAV-assisted sensing of ground targets, discussing the ISAC interactions between UAVs and base stations (BSs). To the best of our knowledge, no existing work has explored the deployment of a collaborative UAV swarm for ISAC purposes while considering imperfect communication between UAVs and realistic wireless channels in the swarm's communication.

Obed Morrison Atsu is with the Engineering Division, New York University (NYU) Abu Dhabi, UAE. Salmame Naoumi is with NYU Tandon School of Engineering, Brooklyn, 11201, NY. Roberto Bomfin is with the Engineering Division, New York University (NYU) Abu Dhabi, UAE. Marwa Chafii is with the Engineering Division, New York University (NYU) Abu Dhabi, UAE and NYU WIRELESS, NYU Tandon School of Engineering, Brooklyn, NY. This work is supported in part by the NYUAD Center for Artificial Intelligence and Robotics, funded by Tamkeen under the Research Institute Award CG010. Authors acknowledge the Technology Innovation Institute (TII) for funding this project.

Inspired by the aforementioned challenges in ISAC systems, this work proposes a novel MARL-based framework to optimize the deployment of UAVs for sensing tasks. The framework strategically optimizes UAV positioning to enhance radar sensing metrics, such as the total achieved sensing signal-to-noise ratio (SNR). The key contributions of this work are summarized as follows:

- We formulate the problem of UAV positioning and path planning as a partially observable Markovian decision process (PO-MDP).
- We introduce a decentralized cooperative MARL approach, enabling UAVs to learn efficient and robust communication protocols, accounting for realistic wireless conditions.
- We enhance the MARL algorithm with a transmission power adaptation mechanism to mitigate inter-carrier interference (ICI) between UAVs and maximize the signal-interference-to-noise ratio (SINR).

The subsequent sections of the paper are organized as follows. In Section II, we introduce the system model for both the sensing ISAC network and the communication network between UAVs. Section III-B formulates the PO-MDP for the optimization problem and presents the MARL algorithm augmented with learned communication. A comprehensive performance analysis is then conducted in Section IV. Finally, Section V provides concluding remarks and insights.

II. SYSTEM MODEL

In this study, we consider a mobile network with K BSs serving users in a predefined area and monitoring q targets. We employ a UAV swarm-enabled ISAC system for broader sensing coverage. In this setup, M UAVs are deployed in a decentralized manner as sensing radars. These UAVs leverage downlink orthogonal frequency division multiplexing (OFDM) symbols from the BSs and repurpose the channel estimation process to estimate the sensing parameters of objects in the environment.

A. Targets sensing channel

From the sensing perspective, the proper trajectory design of each drone in the swarm is the primary factor to enhance the overall sensing performance and therefore optimally covering the designated geographical area. Indeed, at a given time snapshot t , where UAVs are located at $\{\mathbf{p}_m^t\}_{m=1}^M$, the overall sensing performance of the UAV swarm can be measured in terms of the total achieved sensing SNR, expressed as

$$\mathcal{R}^t = \sum_{m=1}^M \sum_{k=1}^K \sum_{i=1}^q \gamma_{m,k}^t(i) \Pi_{m,k}^t(i), \quad (1)$$

where $\gamma_{m,k}^t(i)$ is the sensing SNR of the i^{th} target by the m^{th} UAV exploiting communication signals transmitted by the k^{th} BS, computed as

$$\gamma_{m,k}^t(i) = \mathcal{P}_{tx}^k + \mathcal{G}_{tx}^k + \mathcal{G}_r^m - \mathcal{P}_n + 10 \log_{10} \left(\frac{c^2}{(4\pi)^3 f_c^2} \right) + \sigma_i - 20 \log_{10} (d_{k,i} d_{i,m}),$$

where \mathcal{P}_{tx}^k and \mathcal{G}_{tx}^m represent the transmission power and antenna gain at the k^{th} BS, respectively, \mathcal{G}_r^m is the antenna gain at the m^{th} UAV, \mathcal{P}_n is the average noise power, and c and f_c are the speed of light and carrier frequency, respectively. The SNR is influenced by the radar cross-section (RCS) of the target, denoted by σ_i , modeled as a statistical distribution and measured in dBsm. The distance from the BS to the target, denoted as $d_{k,i}$, and the distance from the target to the UAV, denoted as $d_{i,m}$, are both measured in meters. Moreover, $\Pi_{m,k}^t(i)$ is a binary function indicating whether the i^{th} target can be sensed by the UAV, provided that the resulting SNR is greater than a threshold γ_s . This threshold determines the SNR value above which UAVs can accurately estimate the target sensing parameters. Importantly, each UAV can resolve a specific maximum number of targets at each time step, as their sensing resolution in both delay and angle dimensions is strongly related to the bandwidth and array apertures at both the BSs and UAVs. We denote by q_{\max} the maximum number of targets that each UAV can sense at each time step of the simulation, and accordingly

$$\Pi_{m,k}^t(i) = \begin{cases} 1 & \text{if } \gamma_{m,k}^t(i) \geq \gamma_s, [\gamma_{m,k}^t(i)] \leq q_{\max} \\ 0 & \text{otherwise,} \end{cases}$$

where $[\gamma_{m,k}^t(i)]$ represents the sorted index of the sensing SNR of the link between the i^{th} target and the k^{th} BS, compared to the SNR of all other targets from all other links at the m^{th} UAV at time t . In the simulation, UAVs are deployed for up to T_{\max} time steps. They must collaborate to plan paths and estimate sensing parameters for randomly distributed targets, aiming to maximize the total achieved sensing SNR. Therefore, robust inter-communication among the UAVs is essential for optimal path planning, particularly in a decentralized setup.

B. UAVs communication channels

In our scenario, UAVs operate based on their local observations without a central control unit. Therefore, we assume that the UAVs have the capability to communicate. In fact, inter-UAV communication is crucial for fostering cooperation and sharing environmental knowledge. Effective communication mitigates the limitations of partial observability and enhances sensing accuracy by disseminating information about the environment's topology. Our approach enables UAVs to develop message policies throughout their interactions with the environment, rather than relying on predefined communication protocols. This emergent communication strategy allows UAVs to create their own communication semantics, which are essential for learning effective path planning strategies [11]. Indeed, the UAVs learn to send continuous communication messages, represented as $m_i \in \mathbb{R}^s$, where s is the dimension of the communication protocol. These messages, generated by neural networks (NNs), contain comprehensive information about the current state of the environment and the semantics developed by each UAV, ultimately enhancing the quality of path planning. Additionally, unlike previous studies that assume perfect wireless channels between all UAV pairs, our

Table I: Attenuation as a function of the spectral distance between two channels \mathcal{C}_j and \mathcal{C}_l with carrier indices \tilde{j} and \tilde{l} , respectively.

Spectral Distance $ \tilde{j} - \tilde{l} $	Attenuation (dB)
0	0
1	20
2	40
3	50
4	60
≥ 5 and $\left \frac{f_{\tilde{j}} - f_{\tilde{l}}}{f_{\tilde{j}}} \right \leq 0.05$	95
else	110

research focuses on practical applications with realistic models of UAV communication channels. The transmission process is stochastic and influenced by factors such as network conditions, including path loss, limited shared bandwidth, and interference, as well as the mobility of the UAVs. As a result, messages sent by one UAV may not be received by all others. Therefore, the UAV swarm must learn effective and robust path planning strategies that address the complexities of realistic wireless communication environments.

For the UAVs communication network, we assume that it accommodates all the UAVs, with the total dedicated bandwidth equally divided into M equal-sized overlapping channels. The m^{th} UAV operates on channel \mathcal{C}_m , defined by the carrier frequency $f_{\tilde{m}}$, for the entire flight duration. Furthermore, we consider a non-orthogonal channel partition, which results in ICI between channels in addition to the path loss experienced by the UAVs. Inspired by the settings in both [12] and [13], considering a pair of UAVs, m and j , where the m^{th} UAV is transmitting a message at time step t , the received SINR $\Gamma_{m,j}^t$ at the j^{th} UAV operating on channel \mathcal{C}_j is given by

$$\Gamma_{m,j}^t = \mathcal{P}_r^{j,m,t} - \mathcal{I}_{j,-m}^t - \mathcal{P}_n - 30, \quad (2)$$

where \mathcal{P}_n is the average noise power and $\mathcal{P}_r^{j,m,t}$ is the signal power at the j^{th} UAV transmitted by the m^{th} UAV and is computed as $\mathcal{P}_r^{j,m,t} = \mathcal{P}_t^{m,t} - \mathcal{P}\mathcal{L}_{m,j}^t$, where $\mathcal{P}_t^{m,t}$ is the transmit power of the m^{th} UAV and $\mathcal{P}\mathcal{L}_{m,j}^t$ is the path loss between the pair of UAVs at positions $p_m^t = (x_m^t, y_m^t, z_m^t)$ and $p_j^t = (x_j^t, y_j^t, z_j^t)$, computed as

$$\mathcal{P}\mathcal{L}_{m,j}^t = 68.08 + 22.5 \log_{10}(\|p_m^t - p_j^t\|) + \xi_\sigma,$$

where ξ_σ is a shadow fading term following a Gaussian distribution with zero mean and a standard deviation σ . Furthermore, $\mathcal{I}_{j,-m}^t$ is the interference power from all other UAVs in the network on channel \mathcal{C}_j , given by

$$\mathcal{I}_{j,-m}^t = \sum_{\substack{l=1 \\ l \neq m}}^M \mathcal{P}_r^{j,l,t} - \mathcal{T}(\mathcal{C}_j, \mathcal{C}_l), \quad (3)$$

where $\mathcal{T}(\mathcal{C}_j, \mathcal{C}_l)$ is the power attenuation on channel \mathcal{C}_j with respect to the l^{th} UAV, depending on the spectral distance between the two channels, as detailed in Table I. Furthermore, we define two thresholds, $\Gamma_1 < \Gamma_2$, to evaluate the SINR $\Gamma_{m,j}^t$

between two agents, m and j , during each communication round. Specifically, if $\Gamma_{m,j}^t \geq \Gamma_2$, the message is successfully received and decoded by agent j . If $\Gamma_1 < \Gamma_{m,j}^t < \Gamma_2$, the receiver detects that a message was sent but cannot decode its content. Conversely, if $\Gamma_{m,j}^t < \Gamma_1$, the receiver neither recognizes that a message was transmitted nor decodes it.

III. PROPOSED MARL ALGORITHM

A. PO-MDP formulation

The objective of this proposed framework, as outlined in Section II, is to maximize the sensing SNR of a set of targets within an environment by optimizing the path planning of a UAV swarm consisting of M UAVs, exploiting communication signals from K BSs serving users in the downlink. To address this problem, we introduce an MARL framework where the UAVs, i.e. reinforcement learning (RL) agents, collaboratively learn optimal action policies, specifically path planning strategies, within the simulation environment. Indeed, we mathematically model the environment as a multi-agent finite-horizon decentralized PO-MDP with communication, defined by the tuple $(\mathcal{S}, \mathcal{A}, \mathcal{O}, T, \mathcal{M}, R, T_{\max}, \gamma)$. Here, \mathcal{S} denotes the space of global states of the simulation environment, and $\mathcal{O} = (\mathcal{O}_1, \mathcal{O}_2, \dots, \mathcal{O}_M)$ represents the space of partial observations for each of the UAVs. The action space is defined as $\mathcal{A} = (\mathcal{A}_1, \mathcal{A}_2, \dots, \mathcal{A}_M)$. The stochastic global state transition model is denoted by $T : \mathcal{S} \times \mathcal{A}_1 \times \mathcal{A}_2 \times \dots \times \mathcal{A}_M \rightarrow \mathcal{S}$, and \mathcal{M} represents the communication space. At each time step t , the m^{th} UAV takes an action a_m^t based on its local observation o_m^t and observes the total reward \mathcal{R}^t as defined in Eq. (1). Although actions are taken separately by each agent, all UAVs receive the same collective reward \mathcal{R}^t , which is shared equally across the team, therefore encouraging a cooperative behavior. The UAV aims to learn a communication-based policy $\pi_{(\mathcal{A}^m, \mathcal{M}^m)}^\Theta(\cdot | o_m^t)$, parameterized by learnable parameters Θ , to maximize the expected total cumulative discounted reward corresponding to the overall sum of the targets SNR, determined by the flight time duration T_{\max} and a discount factor $\gamma \in [0, 1]$, and computed as

$$J(\Theta) = \mathbb{E}_{\pi_{(\mathcal{A}, \mathcal{M})}^\Theta} \left[\sum_{t=1}^{T_{\max}} \gamma^{t-1} \mathcal{R}^t \right]. \quad (4)$$

B. MARL architecture

For our MARL framework, we employ a NN architecture to learn communication-based action policies for each UAV in the swarm. These policies are based on both the partial observations of the agents and the messages broadcasted. At time step t , the m^{th} agent receives its local observation o_m^t along with messages from all other agents transmitted at time step $t-1$, denoted as m_{-m}^{t-1} . Here, the notation $-m$ represents the set of all agents except the m^{th} agent. The local observation of each agent comprises its current position (X and Y coordinates) and, for each of the q_{\max} detected targets, their positions, their sensed SNR, and the X and Y coordinates of

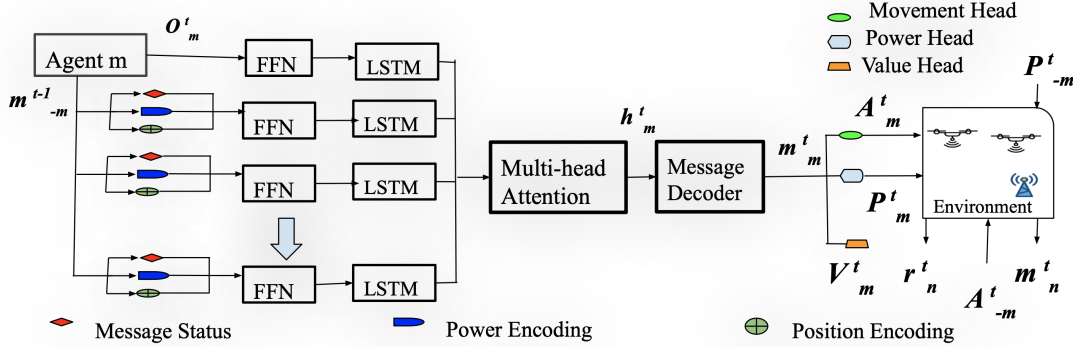


Figure 1: Illustration of the architecture of our proposed MARL algorithm with communication.

the corresponding BSs. Formally, the local observations can be expressed as

$$o_m^t = p_m^t \cup \left(\bigcup_{i=1}^{q_{\max}} \{ \gamma_{m,b_m}^t(i), p_{t_i}^t, p_{b_m}^t \} \right) \in \mathbf{R}^{2+6q_{\max}},$$

where b_m is the index of the BS with the link providing the highest SNR $\gamma_{m,b_m}^t(i)$ for target i . Additionally, p_m^t , $p_{t_i}^t$, and $p_{b_m}^t$ denote the positions of the m^{th} UAV, the i^{th} target, and the corresponding BS, respectively. Furthermore, for each message transmitted by other agents, we account for the possibility that the m^{th} agent may not receive the message. To address this, we construct adapted versions of the messages, where each adapted message consists of the received message or a randomly generated one if the original message cannot be decoded, along with the status of the message, and the index of the transmitting agent. Formally, for agent $j \in -m$, assuming the dimensionality of the transmitted messages is predefined as s , the adapted message $\tilde{m}_j^t \in \mathbf{R}^{s+2}$ is constructed as follows

$$\tilde{m}_j^t = \begin{cases} [m_j^{t-1}, 1, j], & \text{if } \Gamma_{j,m}^t \geq \Gamma_2, \\ [\epsilon, 0, j], & \text{if } \Gamma_1 < \Gamma_{j,m}^t < \Gamma_2, \\ [\epsilon, -1, j], & \text{if } \Gamma_{j,m}^t < \Gamma_1, \end{cases}$$

where $\epsilon \sim \mathcal{N}(0, \mathbf{I})$, and Γ_1 and Γ_2 are the communication SINR thresholds as defined in Section II. As depicted in Fig. 1, a long short-term memory (LSTM)-Attention based architecture [14], [15], similar to [9], is used to enhance the learning of communication-based action policies for the UAV swarm. This architecture outputs a distribution over actions, denoted as $\pi_{(A^m, \mathcal{M}^m)}^\Theta(\cdot | o_m^t)$ for each agent m at time step t , as well as the messages to be transmitted for the subsequent time step. For the m^{th} agent, the partial observation o_m^t is initially encoded using an observation-specific module, which consists of a single-layer feed-forward network (FFN) $\mathbf{o}_{FFN}(\cdot)$ followed by an LSTM module $\mathbf{o}_{LSTM}(\cdot)$. This module maps the partial observation input to an embedding \tilde{o}_m^t of size s , corresponding to the predefined communication message size. Simultaneously, the adapted messages from other agents $\tilde{m}_j^t, \forall j \in -m$ are encoded using a message-specific module, which also includes a single-layer FFN $\mathbf{m}_{FFN}(\cdot)$ and an LSTM

cell $\mathbf{m}_{LSTM}(\cdot)$, mapping the adapted messages to an embedding \tilde{m}_j^t of size s . Subsequently, a multi-head attention block with $M+1$ heads aggregates the observation representation with the encoded messages from other agents. The output of this attention block, denoted as \tilde{h}_m^t , is then fed into a message decoder, a two-layer FFN with a ReLU activation function denoted as $\mathbf{m}_{dec}(\cdot)$. This decoder outputs the outgoing message m_m^t for the next step. This message also serves as an input to both the policy and value heads. Indeed, two policy heads are employed, each composed of an FFN followed by a softmax function to output distributions over the action space. The first policy head, $\pi_{mov}(\cdot)$, is responsible for path planning, outputting a distribution over possible UAV movement actions. In our work, we consider that UAVs operate at a fixed altitude and constant speed ν . Thus, the discrete action space includes movements along the X and Y axes and diagonal movements represented as $\{(\pm\nu, 0), (0, \pm\nu), (\pm\frac{1}{\sqrt{2}}\nu, \pm\frac{1}{\sqrt{2}}\nu)\}$. The second policy head $\pi_{pow}(\cdot)$, serves as a transmission power adaptation mechanism, outputting a distribution over the set of possible communication transmit power levels. At each time step, movement and power level actions $a_m^t = (A_m^t, P_m^t)$ are sampled for each agent from these policy distributions. Additionally, the value head, denoted as $\mathcal{V}(\cdot)$, is an FFN used to estimate the value function V_m^t and serves as a baseline for the MARL algorithm, thereby enhancing the robustness and efficiency of training. A summary of the formalized operations of the architecture is given in **Algorithm 1**. Here, c_m^t and \tilde{c}_j^t are the cell states of the LSTM modules, and they are randomly initialized at $t = 0$, along with the encoded representations \tilde{o}_l^0 and \tilde{c}_l^0 for all agents $l \leq M$. The MultiHead attention operation is defined as $\text{MultiHead}(Q, K, V) = \text{Concat}(\text{head}_1, \dots, \text{head}_{M+1})W^O$ where

$$\text{head}_i = \text{Softmax} \left(\frac{QW_i^Q (KW_i^K)^T}{\sqrt{d_k}} \right) VW_i^V,$$

where d_k is the dimension of the inputs and W^O , W_i^Q , W_i^K , and W_i^V are parameter matrices to be learned. For training, we use the policy gradient method to update the parameters Θ of the architecture, thereby optimizing the reward defined in Eq. (4). Specifically, the parameters of the architecture are

Algorithm 1 Operations of the MARL architecture for the m^{th} UAV at time step t .

- 1: **Input:** $o_m^t, \{m_j^{t-1}\}_{j \in -m}$
- 2: **Observation and Message encoding:**
- 3: $\tilde{o}_m^t, c_m^t = \mathbf{o}_{\text{LSTM}}(\mathbf{o}_{\text{FFN}}(o_m^t), \tilde{o}_i^{t-1}, c_m^{t-1})$
- 4: $\tilde{m}_j^t, \tilde{c}_j^t = \mathbf{m}_{\text{LSTM}}(\mathbf{m}_{\text{FFN}}(\tilde{m}_j^t), \tilde{m}_j^{t-1}, \tilde{c}_j^{t-1}), \forall j \in -m$
- 5: **Multi-Head Attention:**
- 6: $Q, K, V = \tilde{o}_m^t \cup (\cup_{j \in -m} \tilde{m}_j^t)$
- 7: $\tilde{h}_m^t = \text{MultiHead}(Q, K, V)$
- 8: **Message decoding:**
- 9: $m_m^t = \mathbf{m}_{\text{dec}}(\tilde{h}_m^t)$
- 10: **Action selection:**
- 11: $A_m^t \sim \pi_{\text{mov}}(m_m^t), P_m^t \sim \pi_{\text{pow}}(m_m^t)$
- 12: **Value computation:**
- 13: $V_m^t = \mathcal{V}(m_m^t)$

updated by minimizing the following loss function

$$\nabla_{\Theta} \mathcal{L}(\Theta) = \frac{1}{T'_{\text{max}}} \sum_{m=1}^M \sum_{t=1}^{T'_{\text{max}}} \left[-\nabla_{\theta} \left(\log \pi_{\text{mov}} \left(A_m^t \mid o_m^t \right) + \log \pi_{\text{pow}} \left(P_m^t \mid o_m^t \right) \right) \times \left(\mathcal{R}^t - V_m^t \right) + \beta \nabla_{\Theta} \left(\mathcal{R}^t - V_m^t \right)^2 \right],$$

where \mathcal{R}^t is the total achieved SNR reward, and T'_{max} is the number of iterations within a batch. The policy gradient loss function combines both the movement action and transmission power policy losses, along with the value loss, balanced by the coefficient β . Additionally, the architecture parameters are shared across UAVs to improve the training efficiency.

IV. RESULTS

To demonstrate the effectiveness of our proposed approach, we evaluate it on a specific use case focused on monitoring drones within a defined environment. The parameters for this environment are provided in Table II. Additionally, we consider various types of commercial drones and their corresponding RCS distributions, based on the data from [16]. It is worth noting that the results presented in this section are averaged across multiple independent simulation runs to ensure the robustness of the proposed approach.

First, we examine the sensing efficiency of UAVs in environments with varying numbers of targets. The results shown in Fig. 2 illustrate the convergence of the MARL algorithm in terms of the percentage of covered targets out of a varying total number q over training epochs. Remarkably, the algorithm achieves over 70% target coverage in most experiments within a short number of epochs, demonstrating both efficient training and fast convergence. For instance, it requires fewer than 30 epochs to achieve nearly 100% coverage in an environment with 75 targets. In these experiments, the number of deployed UAVs is fixed at 5. The observed performance differences in the final percentage of covered targets are mainly attributed to the spatial distribution of targets within the environment and the constraints imposed by the maximum flight duration, which

Table II: Simulation and Training Parameters.

Simulation Parameter	Value
Environment dimensions ($L \times H$)	1000 × 1000 m ²
Number of iterations (T_{max})	100
UAVs altitude (h)	25 m
UAVs speed (ν)	20 m s ⁻¹
Carrier frequency (f_c)	28 GHz
Shadow fading standard deviation (σ)	3.56 dB
Transmit Power (\mathcal{P}_{tx}^k)	46 dBm
Noise Power (P_n)	-99 dBm
Antenna gains ($\mathcal{G}_{tx} = \mathcal{G}_r$)	11 dBi
Communication SINR thresholds ($\Gamma_1 < \Gamma_2$)	(-10, 0) dB
Sensing SINR threshold (γ_s)	-10 dB
Training Parameter	Value
Discount factor (γ)	0.9
Optimizer	RMSProp
Number of epochs	100
Batch size	5
Learning rate	10 ⁻⁴
Value loss coefficient (β)	0.014

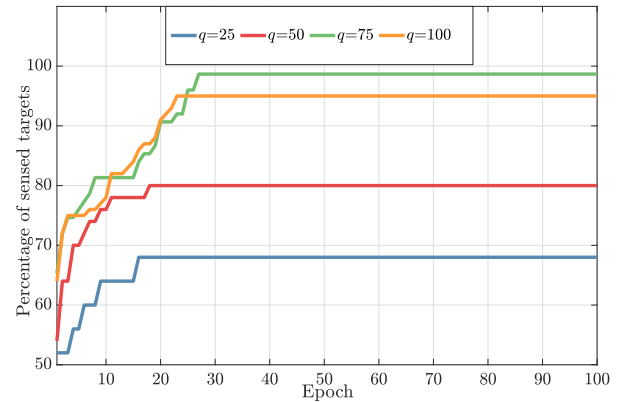


Figure 2: Evolution of the percentage of detected targets by the UAV swarm in environments with the number of targets q .

limit the ability of the UAV swarm to thoroughly explore the environment. Nevertheless, a higher number of targets allows for greater coverage during the planned trajectories of the UAV swarm. Furthermore, we analyze the discounted cumulative reward of all UAVs in environments with varying numbers of UAVs M . In this analysis, the number of targets is set to 100, and the resulting reward is plotted over 100 epochs. The results show that increasing the number of agents ensures that more targets are covered, yielding higher rewards compared to deploying fewer agents. This performance increase is primarily due to the efficient inter-communication incorporated into the MARL algorithm, which maintains coordination among the agents and avoids scalability issues. The trade-off is that the algorithm requires more time to converge with a higher number of agents. However, the algorithm typically needs less than 30 epochs to converge.

Finally, we evaluate the algorithm's ability to learn optimal power levels for each UAV to maintain reliable communication

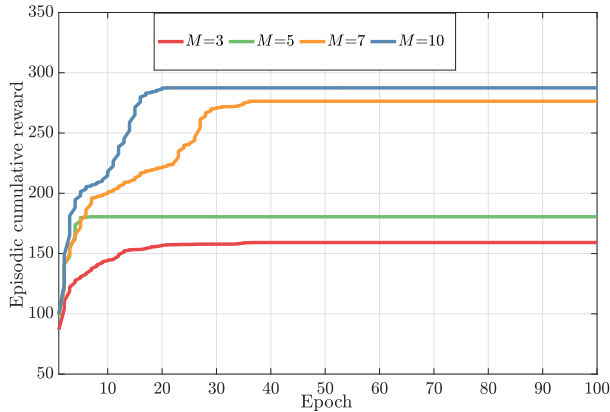


Figure 3: Episodic cumulative reward comparison in environments with increasing UAV number (M).

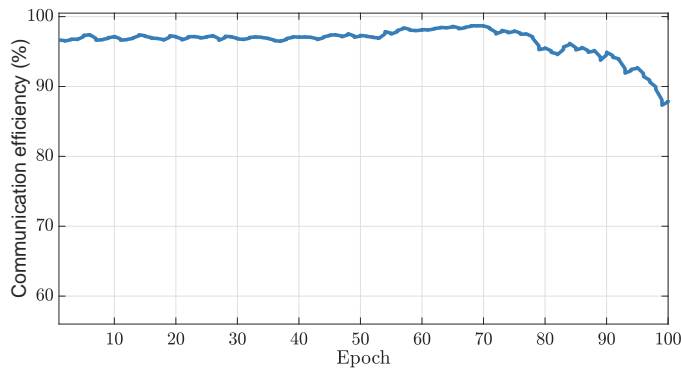


Figure 4: Inter-UAV communication efficiency as the percentage of messages exceeding the SINR threshold.

by ensuring transmitted messages exceed the SINR threshold required for decoding. Fig. 4 shows the percentage of messages surpassing the SINR threshold Γ_2 , indicating successful transmission. The algorithm maintains over 95% efficiency up to the 80th epoch, before dropping to a minimum of 87% by the 100th epoch. This decline occurs when all targets in the environment have been sensed, reducing the need for active UAV communication and movement. Despite this, the algorithm remains robust, effectively balancing power usage based on operational needs. These findings highlight the robust performance of the proposed framework, demonstrating its suitability for ISAC applications and confirming its effectiveness and broad applicability.

V. CONCLUSION

This paper introduced a novel MARL framework for UAV swarm path planning in communication-centric bistatic ISAC applications. Our approach leverages inter-UAV communications to optimize positioning and path planning, thereby enhancing the overall radar sensing performance. The decentralized cooperative framework enables UAVs to develop effective communication protocols, improving their environmental

awareness and operational efficiency. Notably, our framework demonstrates exceptional performance in terms of coverage and overall sensing SNR across various environmental settings, as well as resilience to realistic wireless conditions by adapting to environmental changes and unstable communication links. Additionally, a transmission power adaptation technique ensures robust performance and maximizes SINR for UAV communications. These contributions underscore the framework's robustness, efficiency, and broad applicability for ISAC networks.

REFERENCES

- [1] F. Liu, Y. Cui, C. Masouros, J. Xu, T. X. Han, Y. C. Eldar, and S. Buzzi, "Integrated sensing and communications: Toward dual-functional wireless networks for 6g and beyond," *IEEE Journal on Selected Areas in Communications*, vol. 40, no. 6, pp. 1728–1767, 2022.
- [2] T. Zhang, S. Wang, G. Li, F. Liu, G. Zhu, and R. Wang, "Accelerating Edge Intelligence via Integrated Sensing and Communication," 2022.
- [3] J. Pegoraro *et al.*, "JUMP: Joint Communication and Sensing With Unsynchronized Transceivers Made Practical," *IEEE Transactions on Wireless Communications*, vol. 23, no. 8, pp. 9759–9775, 2024.
- [4] X. Gu and G. Zhang, "A survey on UAV-assisted wireless communications: Recent advances and future trends," *Comput. Commun.*, vol. 208, no. C, p. 44–78, aug 2023.
- [5] J. A. Zhang, M. L. Rahman, K. Wu, X. Huang, Y. J. Guo, S. Chen, and J. Yuan, "Enabling Joint Communication and Radar Sensing in Mobile Networks—A Survey," *IEEE Communications Surveys & Tutorials*, vol. 24, no. 1, pp. 306–345, 2022.
- [6] H. Shakhathreh, A. Khreishah, and B. Ji, "Providing wireless coverage to high-rise buildings using UAVs," in *2017 IEEE International Conference on Communications (ICC)*, 2017, pp. 1–6.
- [7] S. Yang, Z. Shan, J. Cao, Y. Gao, Y. Guo, P. Wang, X. Wang, J. Wang, T. Zhang, and J. Guo, "Path planning of UAV base station based on deep reinforcement learning," *Procedia Computer Science*, vol. 202, pp. 89–104, 2022.
- [8] Y. Jiang, Q. Wu, W. Chen, and K. Meng, "UAV-Enabled Integrated Sensing and Communication: Tracking Design and Optimization," *IEEE Communications Letters*, vol. 28, no. 5, pp. 1024–1028, 2024.
- [9] S. Naoumi, R. Bomfin, R. Alami, and M. Chafii, "TANAGERS: Emergent Communication for UAVs as Flying Passive Radars," in *IEEE WCNC Model-driven DL for 6G IoT*, 2023.
- [10] J. Mu, R. Zhang, Y. Cui, N. Gao, and X. Jing, "Uav meets integrated sensing and communication: Challenges and future directions," *IEEE Communications Magazine*, vol. 61, no. 5, pp. 62–67, 2023.
- [11] M. Chafii, S. Naoumi, R. Alami, E. Almazrouci, M. Bennis, and m. Debbah, "Emergent communication in multi-agent reinforcement learning for future wireless networks," *IEEE Internet of Things Magazine*, vol. 6, pp. 18–24, 12 2023.
- [12] M. Polese, L. Bertizzolo, L. Bonati, A. Gosain, and T. Melodia, "An experimental mmwave channel model for uav-to-uav communications," *CoRR*, vol. abs/2007.11869, 2020.
- [13] Y. Cohen, T. Gafni, R. Greenberg, and K. Cohen, "SINR-Aware Deep Reinforcement Learning for Distributed Dynamic Channel Allocation in Cognitive Interference Networks," *ArXiv*, vol. abs/2402.17773, 2024.
- [14] S. Hochreiter and J. Schmidhuber, "Long short-term memory," *Neural computation*, vol. 9, no. 8, pp. 1735–1780, 1997.
- [15] A. Vaswani, N. M. Shazeer, N. Parmar, J. Uszkoreit, L. Jones, A. N. Gomez, L. Kaiser, and I. Polosukhin, "Attention is All you Need," in *Neural Information Processing Systems*, 2017.
- [16] V. Semkin, J. Haarla, T. Pairon, C. Slezak, S. Rangan, V. Viikari, and C. Oestges, "Analyzing radar cross section signatures of diverse drone models at mmwave frequencies," *IEEE Access*, vol. 8, pp. 48 958–48 969, 2020.